# METEORIX: A CUBESAT MISSION DEDICATED TO THE DETECTION OF METEORS AND SPACE DEBRIS

**N. Rambaux**[(1)], **J. Vaubaillon**[(1)], **L. Lacassagne**[(2)], **D. Galayko**[(2)], **G. Guignan**[(3)], **M. Birlan**[(1)], **P. Boisse**[(4)], **M. Capderou**[(5)], **F. Colas**[(1)], **F. Deleflie**[(1)], **F. Deshours**[(6)], **A. Hauchecorne**[(3)], **P. Keckhut**[(3)], **A.C. Levasseur-Regourd**[(3)], **J.L. Rault**[(7)], **B. Zanda**[(8)], **and all students of the Meteorix team**[(9)]

[(1)] *IMCCE/Paris Observatory, Univ. PSL, Sorbonne Université, CNRS, Paris, France*
[(2)] *LIP6, Sorbonne Université, CNRS, Paris, France*
[(3)] *Sorbonne Université, LATMOS-CNRS, Paris, France*
[(4)] *IAP, Paris, France*
[(5)] *Laboratoire de Météorologie Dynamique, IPSL, Paris, France*
[(6)] *L2E, Paris, France*
[(7)] *International Meteor Organization, Hove, Belgium*
[(8)] *Museum National d Histoire Naturelle, Paris, France*
[(9)] *Sorbonne Université - Campus Pierre et Marie Curie, Paris, France*

## ABSTRACT

We present a university CubeSat space mission dedicated to the detection and characterization of meteors and space debris. The primary objective is to assess a robust statistics of meteoroids and space debris that enter the Earth atmosphere. At present, their fluxes and properties are not yet determined accurately. These estimates will allow us to quantify the delivery of extraterrestrial material on Earth, and possible consequences on aeronomy (e.g. noctilucent clouds and atomic layer). These estimations are also crucial to estimate impact risks for artificial satellites during meteor showers. The knowledge of the flux of space debris will allow us to bring constraints to the space agencies models of space surveillance. There are several secondary objectives, such as bringing information on ablation, fragmentation, rotation processes by studying photometric variations; determining the trajectory in connection with Earth-ground networks such as the Fireball Recovery and InterPlanetary Observation Network (FRIPON) network developed in France in order to find the dynamical origin of the meteoroid; and also detecting other fainter luminous atmospheric phenomena such as luminous transient events. The technological objective is dedicated to the autonomous detection of meteors on board of a CubeSat. This CubeSat is a 3U developed by students at Sorbonne University. The project has validated the feasibility phase.

Keywords: Meteors, Space Debris, Space Mission, cubesat.

## 1. INTRODUCTION

The paper describes a 3U (3U is 30x10x10 cm$^3$) cubesat mission dedicated to the detection of meteors and space debris from space to address the primary question of the flux density of these objects arriving on the Earth that are still puzzling. The meteor detection is an extremely active field with the creation of large Earth-ground camera networks, such as the Canadian, Australian, European networks, and the French Fireball Recovery and InterPlanetary Observation Network (FRIPON) network [7, 8]. However, spaceborne observations present some advantages over the Earth-ground segment namely no weather constraints, long recording time, and wide coverage. Recently, two space projects have been developed with the purpose to detect meteors from space. The S-CUBE cubesat [13] that was launched in 2015 and the Meteor experiment onboard of the International Space Station (ISS). The primary goal of the Meteor experiment is to perform spaceborne observations of chemical composition of the meteors [1]. This experiment, although subject to some constraints because onboard of ISS, has shown the feasibility to observe meteors from space and to appreciate all the difficulty for detection from spaceborne.

Our present mission is called Meteorix and it will carry a camera and a flight detection chain as a minimum payload. It is a simplified version of the previous mission concept based on photometry and UV spectroscopy observations of meteors [26]. In section 2, we discuss the science and the main objectives that drive the Meteorix mission. In section 3, we discuss the mission analysis of the trajectory and measurement strategy and we address a mission design that could be used to realize Meteorix. In section 4, we conclude on the plausibility of this demonstrator.

*Table 1. Scientific requirements for Meteorix mission.*

| Scientific requirement | Description |
|---|---|
| **SR-1** | The Meteorix nanosatellite shall determine meteors apparent visual magnitude between 6 and -10. If magnitude 6 is too low, it is possible to increase at apparent magnitude 3, i.e. absolute magnitude 0 at 500 km altitude. |
| **SR-2** | To perform robust statistics on the entry of meteoroids, the mission shall detect a few hundred meteors. On average, the mission shall detect one meteor per day and 20 meteors during meteor showers. |
| **SR-3** | The nanosatellite mission shall measure all main meteor showers at least one time. |
| **SR-4** | In order to increase the number of detections of faint events the nanosatellite should be able to point straight down at nadir. |
| **SR-5** | The observation shall be performed during the night. |
| **SR-6** | The mission should detect one event with at least 10 frames per second in order to detect the temporal variability of the magnitude. |
| **SR-7** | In order to detect fragmentation, rotation and interaction with the atmosphere, the mission shall measure the luminosity variation of a meteor every 0.1 s with a magnitude accuracy of 0.2. |
| **SR-8** | The mission shall determine the position and record the time of the event in order to reconstruct trajectory and velocity of meteors by combining these data with Earth-ground observations. |
| **SR-9** | The mission shall detect the re-entry of artificial satellites in the Earth atmosphere by imagery. |

## 2. MISSION OBJECTIVES

The terrestrial atmosphere is a natural detector of meteoroids, which arrive on the Earth at a very high speed, and of space debris at the time of their final re-entry. The scientific requirements are provided in Table 1 and details of the objectives are provided below.

**Meteor parent bodies:** The Earth is regularly impacted by meteoroids however the knowledge of the flux density of meteoroids is not yet well constrained [e.g. 16, 28, 35]. The meteoroids come from two reservoirs: comets and asteroids. For the first reservoir, the meteoroids are related to the comet stream that the Earth can cross during its revolution around the Sun. For the second reservoir, the meteoroids are formed by several mechanisms such as the collisions between asteroids, outgassing or by damage of the mineralogical matrix during the heating and cooling phases [14]. The knowledge of the ratio of icy to silicate bodies entering into the terrestrial environment makes it possible to bring some constraints onto the formation of the Solar System (grand-tack model, [33]). The main objective of the Meteorix project is to provide an estimate of the flux of meteoroids arriving on Earth. Such estimation will allow constraining meteorids models like IMEX [30]. A secondary objective is to make a first classification on the nature of objects of asteroidal or cometary origin, from the adjustment of the variation of magnitude with a physical model of meteoroid-atmosphere interaction depending on the physical parameters of the bodies derived from data provided by the demonstrator. These data will also be combined with the multi-technical ground-based data (camera network such as FRIPON and LIDAR data for the atmosphere) to obtain very accurate measurements.

**Space Debris:** Every day satellites, rocket stages and fragments enter into the dense Earth atmospheric layers and even some fragments of these objects can reach the ground. According to [25] and in agreement with the public space debris catalogs, there are about 20,000 debris larger than 10 cm, observed by a global network of telescopes and radars. This estimated number is hundreds of thousands for bodies of 1 to 10 centimeters and several millions or even hundreds of millions for objects less than one centimeter in size. These objects are potentially dangerous for Earth's satellites, because in the event of a collision they can cause severe breakdowns or even the destruction of the satellite and generates lots of debris. In case of manned flights, the consequences can be dramatic. Consequently, it is essential to be able to monitor and study the atmospheric re-entry of space debris as well as the fall on the ground of possible massive objects (such as the Chinese station Tiangong-1 that decayed in 2018). This monitoring and study are particularly important for 1 cm to 10 cm size objects because they are still massive enough to cause significant damage to the space

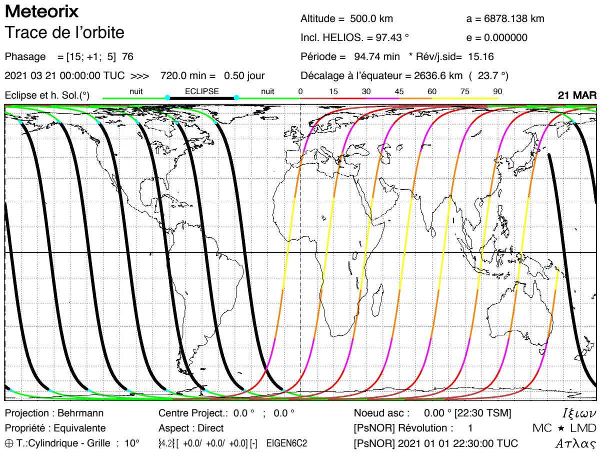


*Figure 1. Ground track of Meteorix mission over 0.5 days. The colors indicate the solar hour and the black curve corresponds to the eclipse time when observations are acquired.*

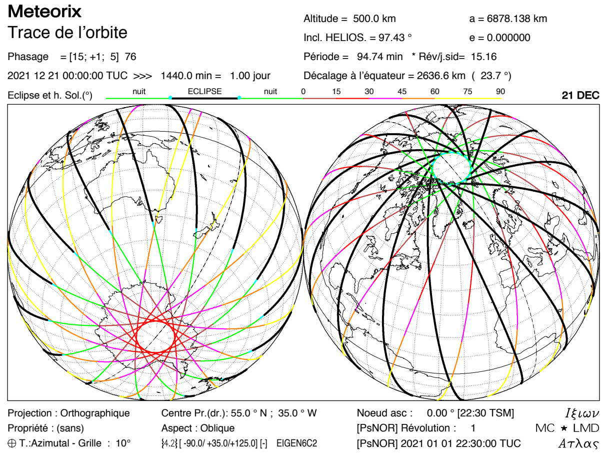


*Figure 2. Ground track of Meteorix mission on a Sun-synchronous orbit over a time span of one day. The Sun-synchronous orbit at 500 km is quasi-polar.*

assets in orbit, while their size makes them virtually undetectable with the currently available observations facilities on the ground (telescopes, radars). The Meteorix project, with its on-board wide-field camera (40 deg), will provide an estimate over time of the flow of space debris entering the Earth's atmosphere, at least along its trajectory. This information is crucial to constrain the spatial distribution patterns of space debris currently developed in space agencies or laboratories.

**Detection chain:** The main challenge of the Meteorix mission is to demonstrate the feasibility of an embedded image processing onboard a cubesat. Indeed the very low power resources available on the cubesat platform places particular constraints on the design of the hardware and software of the detection chain. The detections are classified into three classes: meteors and debris, cities and various areas with stray lights caused by human activities, and others (reflectance of lightning within stormy clouds, stray light from the Moon reflected on the clouds). The chain combines optical flow computation (to detect moving luminous blobs) with morphological and kinematic filtering (based on the apparent speed and its standard deviation). The processing chain is complex due to the requirement of detection robustness and to numerous light disturbances. Consequently, the processing chain has been designed to be tunable to make trade-offs between the detection/classification quality and the embedded criteria (power consumption, processor computing power, sensor size, camera frame rate, available power).

**Formation of future young researchers and engineers:** The project is developed in Sorbonne Université where a large number of students are involved in the project. The objectives are (i) the active engagement and consolidation of the basic theoretical knowledge acquired during academic courses, (ii) the development of methods for problem analysis, synthesis and comparison with various technical solutions in contact with engineers and researchers for feedback and optimization of solutions, (iii) acquisition of complementary skills such as team work, collaborative work, writing of documents for reviews - presentation of journals - taking initiatives; (iv) first contacts with the CubeSat industry.

## 3. MISSION ANALYSIS AND OBSERVATIONAL STRATEGY

The Meteorix payload is a visible camera and its detection chain dedicated to the detection of meteors and space debris. The orbital requirements for the mission are a low Earth orbit to detect faint meteors, to perform good coverage, to observe the dark side of Earth, to conduct a one year mission, and to respect the French space operation law ("loi des opérations spatiales"). The orbital specifications were analyzed by using Celestlab and STELA (CNES softwares dedicated to space mechanics) and the Ixion software [6]. We deduce that a quasi-circular orbit of an altitude of 500 km fits the requirements. We propose a sun-synchronous orbit that is the most common orbit for cubesats and that maximizes the launch date available when the cubesat is ready. Figures 1 and 2 show the spatial coverage of the cubesat over the Earth and the specific colors represent the eclipse period time in black and local solar hour in colors. However, the sun-synchronous orbit imposes a specific choice for the local mean solar time (LMT) related to the ascending node of the orbit [6]. This angle needs to be chosen carefully in order to opti-

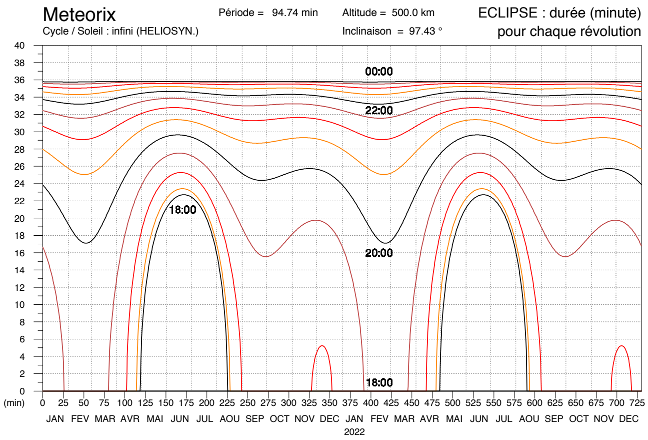


*Figure 3. Duration of solar eclipse in minutes as a function of the day of the year between 2021 and 2022 for various local mean solar times (LMT).*

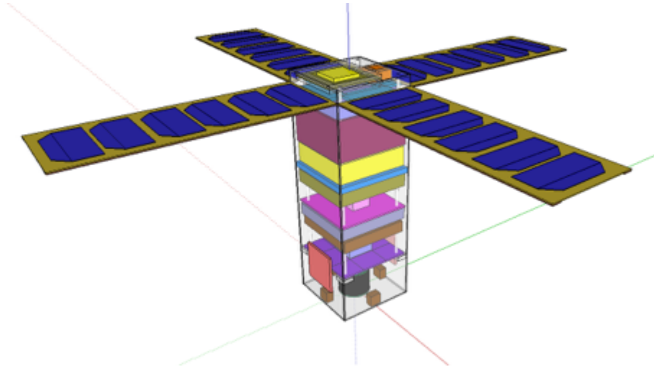

*Figure 4. Design of the Meteorix 3U cubesat.*

mise the observation time. Figure 3 represents the eclipse time for each revolution as a function of the date (2021-2022) for a 500 km altitude orbit. The different curves represent the variations as a function of the LMT angle. In order to optimise the observation time, orbits with

$$10\text{h} < \text{LMT} < 14\text{h} \ \text{ or } \ 22\text{h} < \text{LMT} < 02\text{h} \qquad (1)$$

are the best choices for an eclipse time larger than 32 minutes per orbit.

The nominal lifetime of the planned mission is one year in order to measure the major meteor showers. During that year, the mission must be able to provide a hundred of sporadic events (single meteors), which corresponds on average to an observation of one meteor per day to achieve a robust statistic. During the meteor showers (multiple meteors) the number of detections per day is at most 20 [2]. The objective here is to study the variability of meteoroids during a meteor showers and to determine the radians of the meteor shower.

A preliminary design of the satellite is shown in Figure 4 where the camera is oriented along the long-axis of the cubesat and points towards the nadir. The observational mode is activated as soon as the cubesat is eclipsed by the Earth. In this mode, the camera collects photons coming from meteors and space debris. Figure 5 shows simulation from two meteors distributions of the number of meteors detected per day by a camera having a field of view of 40 to 120 deg with a sensitivity allowing detection of objects of absolute magnitude 0, 2 and 4. The camera is supposed to be at an altitude of 500 km and pointing to the nadir as in Meteorix configuration and the results partly come from the preliminary study of [2]. This figure shows two distributions of meteors: (i) the red curves that comes from the analysis of [27] which favors visual

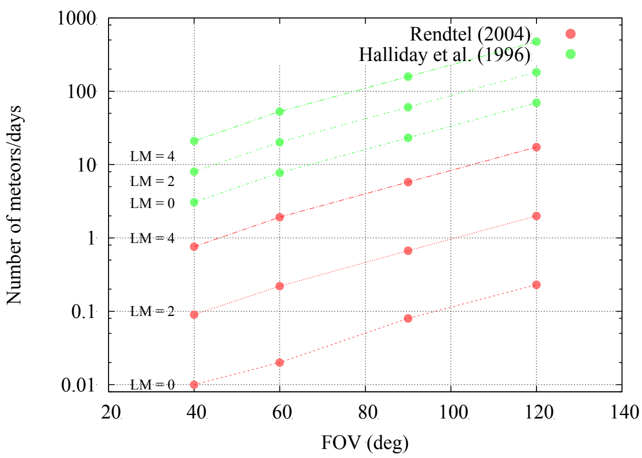


*Figure 5. Number of sporadic events per day as a function of the field of view of the camera for a CubeSat at 500 km altitude. LM represents the detection magnitude limit for two distribution laws: Rendtel 2004 in green [27] and Halliday et al. 1996 [9] in red).*

observations (weak magnitude) and (ii) the second distribution, materialized by the green curves, that comes from the work of [9] which used an automatic and systematic detection system favoring large objects similar to those targeted by our mission. Consequently, the distribution of [9] is used as a reference for our estimates. The principal science objective is to determine the density flux of meteors and the requirement is one meteor per day. Such a requirement is obtained for a field-of-view of 40 deg for detection of meteors of magnitude between 0 and 4 (using the green curves of Figure 5). In addition, we note that the figure shows large differences in the estimates of meteor fluxes, highlighting the need for robust statistics. The observation of the atmospheric re-entry of space debris can be programmed in advance if it concerns cataloged objects, or on the contrary unexpected if it is an object too small to give place to regular observations. According to [21] the re-entry flux of space debris is substantially similar to that of meteors.

The camera will measure the meteors and space debris of apparent visual magnitude between 6 and -10 (see Table 1). In a traditional imagery cubesat mission, such a camera acquires data during the day and the sensitivity of such camera is too low for meteor detection. Consequently, the solution proposed is to adapt a 3D PLUS sensor 3DCM681 with an optical lens of 40 deg of field of view to obtain the camera of Meteorix. Future detailed analysis should validate this strategy. The acquisition of this sensor takes place at a rate of 10 images per second and the size of the image is 1.3 MB (1024x1024 pixels, 10 bits per pixel). For a 3 seconds long single meteor (10 times the mean value of meteor duration), the strategy is to transmit on Earth all the images using the S band (simulations carried out under Celestlab from the CNES library, and taking into account the link budgets). On the other hand, when the meteor time span is longer or during meteor showers with multiple meteor detections, the volume of data is too large to be downloaded to Earth. A processing algorithm will isolate the region of interest from the image containing it. Thus the telecommunication will transmit on Earth only this part of the image.

The acquisition at 10 frames per second makes it possible to exploit the variation in magnitude of the phenomenon of re-entry over time and to classify the meteors according to the dominant physical processes such as ablation, rotation, or fragmentation [31]. Assuming that the meteor or debris is at an altitude of 100 km, it is then possible to relate the variation in magnitude to the physics of the object. However, the combination of the nanosatellite data with ground data from cameras or radars, will provide the 3D trajectory, the speed of entry, the altitude of the meteor, and connection with the physics of the meteor to the origin of the meteoroid [32].

The processing chain consists in detecting bright moving spots and filtering all the spots to classify them into three categories: meteors or debris, cities and related areas, and others (reflectance of lightning within stormy clouds, stray light from the Moon reflected on the clouds ). Illustrations of the method are shown in Figures 6 (a,b,c). The apparent speed of each pixel is estimated with the optical flow of Horn-Schunck algorithm [12]. The gray-level image is binarized with the Otsu algorithm [20], then the binary image is labeled with a connected component labeling and analysis algorithm [29] to cluster pixels into blobs (connected component) all connex pixel. A first morphological filter (based on the shape of the blobs) removes the too small and too big blobs. The average speed and its standard deviation are then computed for every remaining blobs. Blobs with an average speed close to the Earth speed (computed as the average of the background) are identified as cities and then removed. Finally, blobs with a small speed standard deviation are classified as meteors (or debris) while those with a high standard deviation are classified as others. In order to achieve real-time processing (that is to process data at the same camera frame rate), many software and algorithmic optimizations shall be performed. First, all the available parallelism inside the processor should be used, so all the algorithms are multi-threaded to use all available cores (up to 4 on lastest ARM Cortex processors) but also SIMDized by handwriting SIMD (Single Instruction Multiple Data) instructions with ARM Neon multimedia extension. If the compiler can easily vectorize trivial algorithms, it cannot do it for complex ones or inefficiently. But this is not enough, because if multicore SIMD processors have much more computation power than classic ones, such a power is limited by the bandwidth of the bus connecting the memory containing the images with the processor. Naive implementation of such a kind of algorithms are memory bound because their arithmetic intensity (the ratio between the number of operations divided by the number of memory accesses) is too low. One has to do High Level Transforms (that are by definition still out of the capabilities of an optimizing compiler) [18, 34]. It consists in transforming the code to avoid memory access, by fusionning the operators composing the algorithms or pipelining them to increase the persistence of data within the caches, and so avoid access to data within the external memory. Such transforms and optimizations have been applied to the optical flow for ARM Cortex A with Neon and also for Nvidia GPU [22, 23]. Concerning connected component labeling [3, 10], the Light Speed Labeling [19] has been used in its parallel implementation [5] for targeting ARM multi-core CPU and a new labeling algorithm inspired by previous ones [4, 15, 17, 24] has been designed for GPU [11]. These algorithms outperform the State-of-the-Art at least by a factor two.

From satellite system point of view, the camera monitors the Earth's atmosphere. The storage system is activated when a luminous phenomenon corresponding to an atmospheric re-entry is detected. The processing chain combines optical flow estimation, connected component labeling and analysis to filter every luminous blob that is detected. Thanks to the connected component analysis, the bounding box (bounding rectangle) of each blob is computed on-the-fly and only such regions of interest that contain the meteor or debris is stored in memory. The optical flow computation performs better for small motions estimation and 20 or 25 frames/s are usually optimal but lower frame rate around 10 frames/s will

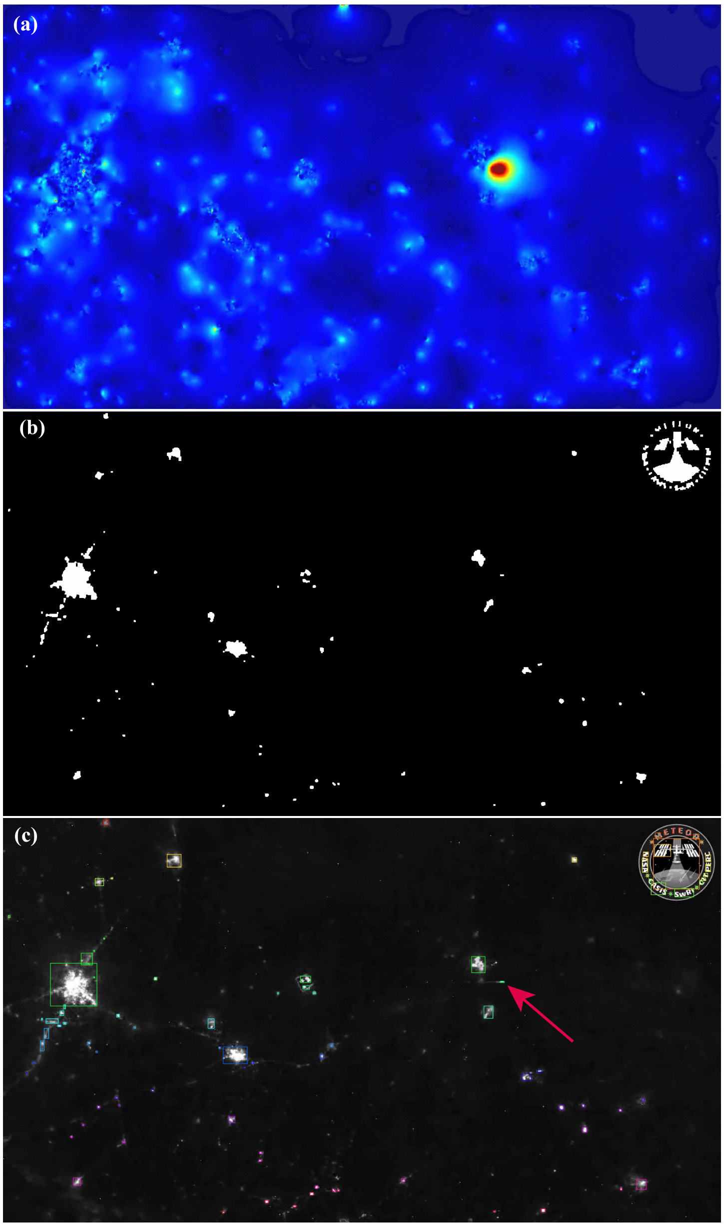


*Figure 6. Example of detection chain applied to a sequence provided by Meteor experiment (Courtesy of T. Arai). (a) Heatmap of the norm of the optical flow (blue for background, red for fast moving blobs. (b) Binary image after binarization and morphological opening (to make very small blobs and single bad pixel disappear): only the remaining white blobs are labeled and analyzed in the next steps of the processing chain. (c) Bounding boxes after the connected component labeling and analysis but before kinematic filtering. After kinematic filtering, the detection chain points towards the meteor/debris (represented with a red arrow) and the cities and others are discarded.*

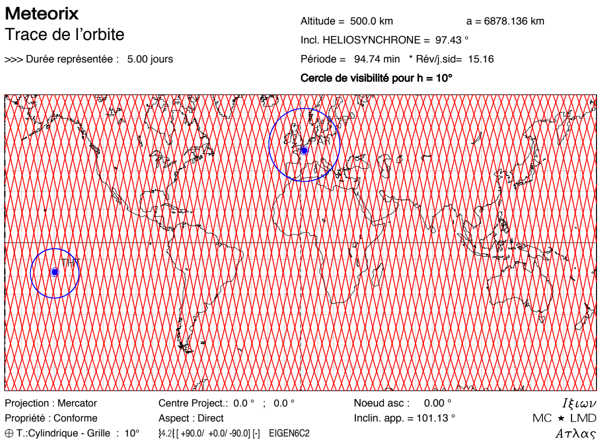


*Figure 7. Ground track of Meteorix mission and visibility circle for Paris and Tahiti over 5 days.*

be evaluated in the future. Some estimations obtained by varying the number of events (sporadic and meteor showers), the event duration, the size of the event (meteor, debris), the camera frame rate, the sensor size, the lense focal for video sequences acquired onboard ISS by the camera of Meteor experiment [1], confirm that, even in the worst case (showers and long duration and high frame rate) all the regions of interest can be stored in the memory of available electronic board for one orbit duration. This treatment chain and its optimizations for a CubeSat are designed by the ALSOC team of "Laboratoire d'Informatique de Paris 6" (LIP6).

The platform is a 3U CubeSat shown in Figure 4 with all necessary vital functions. Preliminary design has been proposed during the feasibility review; it needs to be detailed for future studies. The solar panels are deployable in order to increase the energy available onboard. The proposed telecommunication sub-system of Meteorix is composed of a UHF band downlink, VHF band uplink, and S band downlink. The UHF/VHF bands will be used for the command and house keeping data whereas the S-band is used to download scientific data. A UHF/VHF ground station has been built at Sorbonne University at Pierre et Marie Curie campus and it is driven by the "Laboratoire d'Électronique et Électromagnétisme" (L2E). Figure 7 shows the passage time of Meteorix over two stations at Paris and at Tahiti over 5 days. The visibility time is better for stations at high latitude as it is shown in the figure. The operational strategy presented before allows to transmit the required scientific data (Table 1) in the link budget.

## 4. CONCLUSION

Meteorix is a space mission designed for a CubeSat 3U that has been proposed inside the Centre Spatial Universitaire, CurieSat, of Sorbonne Université. It is a demonstrator for the detection and characterization of meteors and space debris from space that could help the development of a future constellation dedicated to the awarness of space debris and large bolides such as the Tchelyabinsk event, and/or to improve meteor science feedback by determining of accurate trajectory and to measure UV spectrum of meteors. The project passed a feasibility review in 2017 defended by the students of the project. It is a great source of motivation and inspiration for young students, as the science is accessible and associated with fascinating challenges and NewSpace developments.

## ACKNOWLEDGMENTS

The authors acknowledge supports from Janus CNES, labex ESEP, DIM-ACAV+ Région Ile-de-France, and the IDEX Sorbonne Universités. The authors wish to thank Tomoko Arai from the PERC project in Chiba University for video sequences, and we particularly thank A. Gaboriaud for sharing his knowledge of CubeSats and students formation.

## REFERENCES

1. Arai, T., Kobayashi, M., Yamada, M., Senshu, H., Maeda, K., Wada, K., Ohno, S., Ishibashi, K., Ishimaru, R., Matsui, T., and Fortenberry, M. (2018). On-Going Status of METEOR Project Onboard the International Space Station. In *Lunar and Planetary Science Conference*, volume 49 of *Lunar and Planetary Inst. Technical Report*, page 2525.
2. Bouquet, A., Baratoux, D., Vaubaillon, J., Gritsevich, M. I., Mimoun, D., Mousis, O., and Bouley, S. (2014). Simulation of the capabilities of an orbiter for monitoring the entry of interplanetary matter into the terrestrial atmosphere. *Planetary and Space Science*, 103:238–249.
3. Cabaret, L. and Lacassagne, L. (2014). What is the world's fastest connected component labeling algorithm ? In *IEEE International Workshop on Signal Processing Systems (SiPS)*, pages 97–102.
4. Cabaret, L., Lacassagne, L., and Etiemble, D. (2017). Distanceless label propagation: an efficient direct connected component labeling algorithm for GPUs. In *IEEE International Conference on Image Processing Theory, Tools and Applications (IPTA)*, pages 1–8.
5. Cabaret, L., Lacassagne, L., and Etiemble, D. (2018). Parallel Light Speed Labeling for connected component analysis on multi-core processors. *Journal of Real Time Image Processing*, 15(1):173–196.

6. Capderou, M. (2014). *Handbook of satellite orbits*. Springer.

7. Colas, F., Baillié, K., Bouley, S., Zanda, B., Vaubaillon, J., Jeanne, S., Egal, A., Vernazza, P., Gattacceca, J., Birlan, M., Baratoux, D., Sylla, S., Jorda, L., Rault, J.-L., Caminade, S., Delcroix, M., Maquet, L., Blanpain, C., Steinhauser, A., Lecubin, J., and Malgoyre, A. (2018). FRIPON and IMPACT projects to pinpoint interplanetary matter in the centimetre - hundred meter range. *European Planetary Science Congress*, 12:EPSC2018–1105.

8. Colas, F., Zanda, B., Bouley, S., Vernazza, P., Gattacceca, J., Vaubaillon, J., Marmot, C., Kwon, M., Audureau, Y., and Rotaru, M. (2014). FRIPON, a French fireball network for the recovery of both fresh and rare meteorite types. In Muinonen, K., Penttilä, A., Granvik, M., Virkki, A., Fedorets, G., Wilkman, O., and Kohout, T., editors, *Asteroids, Comets, Meteors 2014*.

9. Halliday, I., Griffin, A. A., and Blackwell, A. T. (1996). Detailed data for 259 fireballs from the Canadian camera network and inferences concerning the influx of large meteoroids. *Meteoritics and Planetary Science*, 31:185–217.

10. He, L., Ren, X., Gao, Q., Zhao, X., Yao, B., and Chao, Y. (2017). The connected-component labeling problem: a review of state-of-the-art algorithms. *Pattern Recognition*, 70:25–43.

11. Hennequin, A., Meunier, Q. L., Lacassagne, L., and Cabaret, L. (2018). A new direct connected component labeling and analysis algorithm for GPUs. In *IEEE International Conference on Design and Architectures for Signal and Image Processing (DASIP)*, pages 1–6.

12. Horn, B. K. P. and Schunk, B. G. (1981). Determining optical flow. *ACM Computing Surveys (CSUR)*, 17(1-3):185–203.

13. Ishimaru, R., Sakamoto, Y., Kobayashi, M., Fujita, S., Gonai, T., Senshu, H., Wada, K., Yamada, M., Kurosawa, K., Hosokawa, S., Yoshida, K., Sato, M., Takahashi, Y., and Matsui, T. (2014). CubeSat Mission for UV-Visible Observations of Meteors from Space: S-CUBE (S3: Shootingstar Sensing Satellite). In *Lunar and Planetary Science Conference*, volume 45 of *Lunar and Planetary Inst. Technical Report*, page 1846.

14. Jewitt, D., Hsieh, H., and Agarwal, J. (2015). *The Active Asteroids*, pages 221–241.

15. Komura, Y. (2015). Gpu-based cluster-labeling algorithm without the use of conventional iteration: application to swendsen-wang multi-cluster spin flip algorithm. *Computer Physics Communications*, pages 54–58.

16. Koschny, D., Albin, T., Drolshagen, E., Drolshagen, G., Drolshagen, S., Koschny, J., Kretschmer, J., van der Luijt, C., Molijn, C., Ott, T., Poppe, B., Smit, H., Svedhem, H., Toni, A., de Wit, F., and Zender, J. (2015). Current activities at the ESA/ESTEC Meteor Research Group. In Rault, J.-L. and Roggemans, P., editors, *International Meteor Conference Mistelbach, Austria*, pages 204–208.

17. Lacassagne, L., Cabaret, L., Hebache, F., and Petreto, A. (2016). A new SIMD iterative connected component labeling algorithm. In *ACM Workshop on Programming Models for SIMD/Vector Processing (PPoPP)*, pages 1–8.

18. Lacassagne, L., Etiemble, D., Hassan-Zahraee, A., Dominguez, A., and Vezolle, P. (2014). High level transforms for SIMD and low-level computer vision algorithms. In *ACM Workshop on Programming Models for SIMD/Vector Processing (PPoPP)*, pages 49–56.

19. Lacassagne, L. and Zavidovique, B. (2011). Light Speed Labeling: Efficient connected component labeling on RISC architectures. *Journal of Real-Time Image Processing*, 6(2):117–135.

20. Otsu, N. (1979). A threshold selection method from gray-level histograms. *Transactions on System, Man and Cybernetics*, 9:62–66.

21. Pardini, C. and Anselmo, L. (2017). Revisiting the collision risk with cataloged objects for the Iridium and COSMO-SkyMed satellite constellations. *Acta Astronautica*, 134:23–32.

22. Petreto, A., Hennequin, A., Koehler, T., Romera, T., Fargeix, Y., Gaillard, B., Bouyer, M., Meunier, Q., and Lacassagne, L. (2018a). Comparaison de la consommation énergétique et du temps d'exécution d'un algorithme de traitement d'images optimisé sur des architectures SIMD et GPU. In *Compas*.

23. Petreto, A., Hennequin, A., Koehler, T., Romera, T., Fargeix, Y., Gaillard, B., Bouyer, M., Meunier, Q., and Lacassagne, L. (2018b). Energy and Execution Time Comparison of Optical Flow Algorithms on SIMD and GPU Architectures. In *IEEE*, International Conference on Design and Architectures for Signal and Image Processing.

24. Playne, D. P. and Hawick, K. (2018). A new algorithm for parallel connected-component labelling on GPUs. *IEEE Transactions on Parallel and Distributed Systems*.

25. Prevereaud, Y. (2014). *Contribution à la modélisation de la rentrée atmosphérique des débris spatiaux. Modélisation et simulation.* . PhD thesis, Institut Supérieur de l'Aéronautique et de l'Espace (ISAE).

26. Rambaux, N., Galayko, D., Mariscal, J.-F., Breton, M.-A., Vaubaillon, J., Birlan, M., Colas, F., and Fouchet, T. (2014). Detection of spectral UV from meteors by a nanosatellite. In Rault, J.-L. and Roggemans, P., editors, *Proceedings of the International Meteor Conference, Giron, France, 18-21 September 2014*, pages 182–184.

27. Rendtel, J. (2004). The population index of sporadic meteors. In Triglav-Čekada, M. and Trayner, C., editors, *Proceedings of the International Meteor Conference, 22nd IMC, Bollmannsruh, Germany, 2003*, pages 114–122.

28. Rendtel, J. and R., A. (2014). *Handbook for Meteor Observers*. International Meteor Organization, Postdam.

29. Rosenfeld, A. and Platz, J. (1966). Sequential operator in digital pictures processing. *Journal of ACM*, 13,4:471–494.

30. Soja, R. H., Sommer, M., Herzog, J., Srama, R., Grün, E., Rodmann, J., Strub, P., Vaubaillon, J., Hornig, A., and Bausch, L. (2014). The Interplanetary Meteoroid Environment for eXploration - (IMEX) project. In Rault, J.-L. and Roggemans, P., editors, *Proceedings of the International Meteor Conference, Giron, France, 18-21 September 2014*, pages 146–149.

31. Čapek, D. and Borovička, J. (2017). Ablation of small iron meteoroids-First results. *Planetary and Space Science*, 143:159–163.

32. Vaubaillon, J., Koten, P., Margonis, A., Toth, J., Rudawska, R., Gritsevich, M., Zender, J., McAuliffe, J., Pautet, P.-D., Jenniskens, P., Koschny, D., Colas, F., Bouley, S., Maquet, L., Leroy, A., Lecacheux, J., Borovicka, J., Watanabe, J., and Oberst, J. (2015). The 2011 Draconids: The First European Airborne Meteor Observation Campaign. *Earth Moon and Planets*, 114:137–157.

33. Walsh, K. J., Morbidelli, A., Raymond, S. N., O'Brien, D. P., and Mandell, A. M. (2011). A low mass for Mars from Jupiter's early gas-driven migration. *Nature*, 475:206–209.

34. Ye, H., Lacassagne, L., Falcou, J., Etiemble, D., Cabaret, L., and Florent, O. (2013). High level transforms to reduce energy consumption of signal and image processing operators. In *IEEE International Workshop on Power and Timing Modeling, Optimization and Simulation (PATMOS)*, pages 247–254.

35. Zolensky, M., Bland, P., Brown, P., and Halliday, I. (2006). *Flux of Extraterrestrial Materials*, pages 869–888.